Thermal-hydraulic-mechanical (THM) modeling of high-temperature heat storage using DeepStor as a case study

Kai Stricker[1], Robert Egert[1], Jens C. Grimmer[1], Maziar Gholami Korzani[2], Eva Schill[3], Thomas Kohl[1]

[1]Institute of Applied Geosciences, Karlsruhe Institute of Technology (KIT), Adenauerring 20b, 76131 Karlsruhe, Germany

[2]School of Civil & Environmental Engineering, Queensland University of Technology, 2 George St Brisbane, QLD 4000, Australia

[3]Institute of Nuclear Waste Disposal, Karlsruhe Institute of Technology (KIT), Herrman-von-Helmholtz-Platz 1, 76344 Eggenstein-Leopoldshafen, Germany

kai.stricker@kit.edu

Keywords: HT-ATES, seasonal energy storage, depleted oil reservoir, THM modeling, poro- and thermoelasticity, uplift

ABSTRACT

Aquifer thermal energy storage (ATES) offers the possibility to store excess heat available in summer, so that it can be used in winter, when the heat demand is higher. In contrast to near-surface aquifer storage, high-temperature ATES allows the exploitation of deeper reservoirs with higher storage temperatures, enabling to meet the demand of industrial processes or district heating systems.

Various studies have been conducted to investigate the performance of ATES systems with regard to their efficiency by using thermohydraulic modelling. Here, we extend these models by deploying coupled thermal-hydraulic-mechanical models to investigate the impact of cyclic high-temperature heat storage on displacements in the reservoir and on the surface. Our results show that moderate flow rates only lead to sub-mm displacements at the surface. The main cause for these displacements is poroelasticity due to injection- and production-related pressure changes within the reservoir. Thermoelasticity plays only a minor role for the observed displacements at the surface but strongly affects the displacements within and close to the reservoir.

1. INTRODUCTION

Nearly 50 % of German CO_2 emissions are related to the provision of building and process heat (Ausfelder et al. 2017). Due to seasonal fluctuations in demand, especially to heat buildings (IEA 2017, REN21 2019), the possibility of local storage of surplus heat in summer, which can be extracted from storage in winter, is becoming increasingly important (Lee 2013). With the current state of technology and foreseeable developments, significant amounts of heat can only be stored underground, taking advantage of the large available storage volumes (Lee 2013). In contrast to near-surface aquifer storage (ATES: Aquifer Thermal Energy Storage; Dickinson et al. 2009), much larger thermal energies can be stored in deep heat reservoirs due to significantly higher injection temperatures (Wesselink et al. 2018).

In a previous study, the high potential of former hydrocarbon reservoirs in the Upper Rhine Graben for high-temperature heat storage has been shown by generic thermal-hydraulic modeling (Stricker et al. 2020). For the safe operation of high-temperature heat storage systems, coupled mechanical processes also cannot be neglected. This has only rarely been done so in the past, mainly focussing on surface uplift caused by poroelasticity (Birdsell and Saar 2020) or the influence of thermo- and poroelasticity on the storage efficiency (Jin et al. 2020).

On the basis of the aforementioned study, we use the DeepStor project as a case study to investigate the impact of coupled mechanical processes on high-temperature heat storage. DeepStor is a planned scientific infrastructure designed to demonstrate the concept of HT-ATES targeting former hydrocarbon reservoirs. The infrastructure is located near Karlsruhe in the Upper Rhine Graben, an area which shows the highest measured thermal anomalies in Germany with temperatures up to 140°C in 2 km depth (Baillieux et al. 2013).

We deploy a generic 3D thermal-hydraulic-mechanical (THM) model derived and simplified from a subsurface model of the DeepStor site to investigate the impact of cyclic seasonal injection and production on the stress distribution in the subsurface and thereby caused displacements in the reservoir and at the surface. Hereby, we focus on a one well setup where the same

well is used for injection of hot water in summer and the production in winter.

2. CONCEPTUAL MODEL

The THM modelling conducted in this paper is based on a structural model of the subsurface of the DeepStor site. The subsurface of the area of interest comprises slightly inclined geological units within a graben system that are constrained by large-scale normal faults. Most units consist of low-permeable clays that are interbedded with fluvial and marine sand-rich or sand layers (Böcker 2015, Bruss 2000, Wirth 1962). The conceptual model derived from the structural model simplifies these interbedded layers by only considering one potential reservoir layer, the Meletta beds. All other layers were lumped together as impermeable cap rock layers with homogeneous parametrization. Also for further simplification, a horizontal geometry was used instead of inclined model layers. The reservoir material properties (e.g. porosity, permeability, or the Young's modulus) were chosen based on available literature for the storage site if available (REF). Operating data (e.g. the flow rate or the injection temperature) were selected based on the planned operational framework of the DeepStor storage site.

The modelling concept is assuming a single well seasonal HT-ATES system with semi-annual injection and production load-time-functions. The well serves both as injector of hot water in summer as well as producer in winter. This type of modelling approach – in contrast to widely used well doublets (e.g. Gao et al. 2017) – is used to demonstrate the maximum potential poro- and thermoelastic impact on the reservoir and especially the surface, serving as a "worst case" szenario. A transient modelling approach is used as steady-state conditions cannot be reached within the modelling timeframe due to low thermal diffusivities of rock.

3. NUMERICAL MODEL

The mass transport equation used to estimate the pore pressure, p, is given by mass balance along with the Darcy velocity, q, as follows (Bear 1972):

$$S_m \frac{\partial p}{\partial t} + \nabla q = Q \qquad [1]$$

$$q = \frac{k}{\mu}(-\nabla p + \rho_f g) \qquad [2]$$

S_m is the mixture specific storage coefficient of the medium, t is the time, Q is the source/sink term for injection and production, k is the permeability tensor, μ and ρ_f are the fluid dynamic viscosity and density, respectively, and g is the gravitational acceleration.

It is assumed that the solid and liquid phases are in local thermodynamic equilibrium. Heat transport used to estimate temperature can be mathematically expressed using the advection-diffusion equation as:

$$\rho c_p \frac{\partial T}{\partial t} - \lambda_b \nabla^2 T + \left(\rho c_p\right)_f q \nabla T = 0 \qquad [3]$$

ρc_p and λ_b are the heat capacity and thermal conductivity of the mixture, respectively. $(\rho c_p)_f$ represents the heat capacity of the fluid.

Deformation of a fully saturated porous medium is described by the momentum balance equation (Jaeger et al. 2009):

$$\nabla \cdot (\sigma' - \alpha p I) + \rho_s g = 0 \qquad [4]$$

σ′ is the effective stress tensor, depending on the total Cauchy's stress tensor σ, the Biot's coefficient α and pore pressure p:

$$\sigma' = \sigma + \alpha p I \qquad [5]$$

Eq. [5] illustrates how deformation is coupled with fluid flow. The constitutive law for stress-strain behaviour links the displacement vector u, the primary variable solved for deformation of the porous medium, to the effective stress tensor σ′:

$$\Delta\sigma' = \mathbb{C}(\Delta\epsilon - \tfrac{1}{3}\beta_d \Delta T I) \qquad [6]$$

$$\epsilon = \tfrac{1}{2}(\nabla u + (\nabla u)^T) \qquad [7]$$

$\mathbb{C}$ is the elastic material tensor, ϵ the strain, β_d the volumetric drained thermal expansion coefficient, and ΔT the temperature change. In this paper, only isotropic, non-isothermal elastic deformation is considered. Therefore, linear elasticity can be fully described by the generalized Hooke's law as:

$$\mathbb{C} = \lambda \delta_{ij} \delta_{kl} + 2\mu \delta_{ik} \delta_{jl} \qquad [8]$$

δ is the Kronecker delta, μ the shear modulus, and λ the Lamé constant.

Equations [1] – [8] are solved deploying the open-source code TIGER (THMC sImulator for Geoscientific Research; Gholami Korzani et al. 2020), which is implemented within the object-oriented framework MOOSE (Permann et al. 2020).

The numerical model extends over 12.5 x 12.5 x 1.6 km with a 10 m thick reservoir at a depth of 1200 m (Fig. 1), resembling and simplifying the subsurface of the DeepStor project. The lateral extent of the model is chosen to avoid any boundary effects, especially on the pressure and displacement fields. The well is located in the centre of the model, vertically exploiting the reservoir. The parametrization (material properties and operating data) used in the model are shown in Table 1.

The unstructured mesh consisting of tetrahedral elements was created using the Gmsh software (Geuzaine and Remacle 2009). The size of the elements ranges from 1 m in the surrounding of the well to 250 m at the model boundaries. A mesh sensitivity analysis was performed to avoid any mesh dependency on the results. In total, the mesh contains 137'599 nodes, connected by 804'642 elements.

Table 1: Parametrization of the model. The hydraulic, thermal and operational parameters are derived from Stricker et al. (2020). The mechanical parameters are based on Marschall and Giger (2014) and Jahn et al (2016).

Parameter	Value
Reservoir permeability [m²]	2.5×10^{-14}
Permeability of the cap rock [m²]	10^{-18}
Porosity (reservoir / cap rock) [-]	0.15
Injection/production flow rate [Ls^{-1}]	1
Injection temperature [°C]	140
Thermal conductivity (reservoir / cap rock) [$W.m^{-1}K^{-1}$]	2.5 / 1.4
Volumetric heat capacity (reservoir / cap rock) [$MJ.m^{-3}K^{-1}$]	3.15 / 3.3
Fluid thermal conductivity [$W.m^{-1}K^{-1}$]	0.65
Fluid specific heat capacity [$J.kg^{-1}K^{-1}$]	4194
Fluid density [$kg.m^{-3}$]	1000
Fluid dynamic viscosity [Pa.s]	4.18×10^{-4}
Fluid bulk modulus [GPa]	2
Rock Young's modulus [GPa]	10
Poisson's ratio [-]	0.25
Biot coefficient [-]	1

Hydrostatic pore pressure and a temperature gradient of 50 $K.km^{-1}$ are applied to the model by setting Dirichlet boundary conditions (BCs) at the top and the bottom of the model with associated initial conditions (ICs). No-flux Neumann BCs are applied to the side planes of the model. No prior stress state is applied to the model, the bottom and the side planes of the model were fixed in normal directions by setting no-displacement Dirichlet BCs (rollers). Injection and production flow are implemented by using semi-annually activated Dirac kernels. To implement the hot water injection during summer, a Dirichlet BC is activated at the top of the well during the injection period.

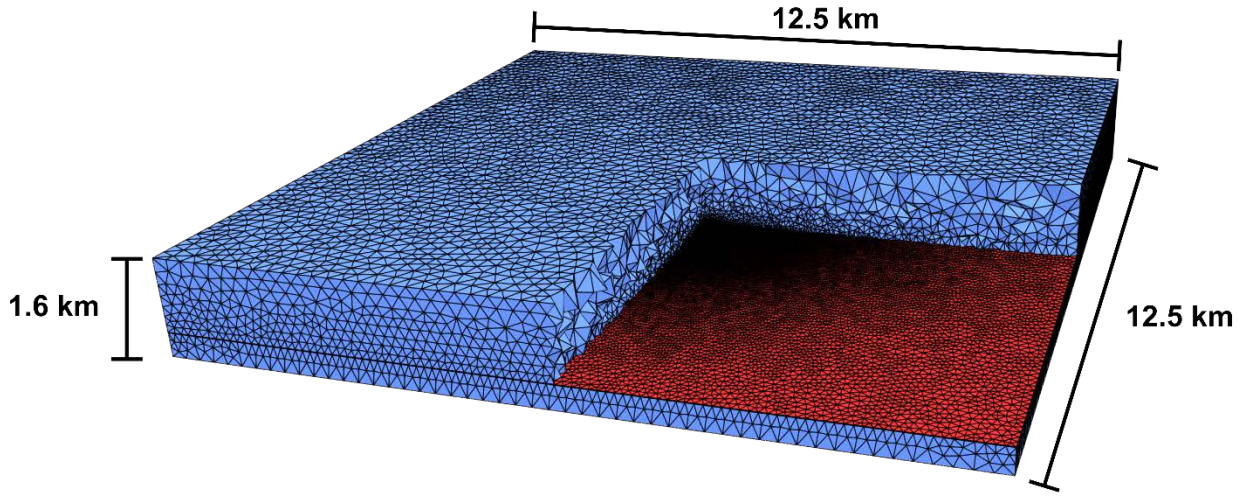

Figure 1: Simplified numerical model of the planned HT-ATES site of the DeepStor project. The model consists of a 10 m thick reservoir (red), confining layers above and below the reservoir (blue), and a well in the centre of the model.

4. RESULTS

To investigate the mechanical response to the injection of hot fluid, a model with the parametrization shown in Table 1 has been simulated over an injection period of six months. It can be seen that this injection results in an uplift of ca. 4.2 mm at the top of the reservoir (Figure 2a). The uplift is sharply concentrated around the injection well and reduces towards the model boundaries where nearly no uplift occurs. At the surface, only ca. 0.24 mm uplift remain, however, showing an impact on a larger area with the uplift trending towards zero at distances greater 4 km (Figure 2b).

The shown uplifts at the reservoir and the surface of the model are caused by the superposition of poroelasticity and thermoelasticity. To separate these two mechanisms and their impact on injection-related uplift, a second model has been simulated, which only considers hydraulic and mechanical processes. Figure 2c shows that the majority of the uplift at the top of the reservoir (ca. 4.2 mm) is related to thermoelasticity and only an uplift of ca. 0.6 mm is caused by poroelasticity. However, the stronger uplift caused by thermoelasticity affects only a small area around the well, which is heated up by the injected hot fluid. This area has a radius of ca. 50 m, resembling the thermal front of the hot water injection. At greater distances to the injection well, the uplift is purely caused by poroelasticity and dissipates slowly towards the model boundaries.

In contrast, the propagated uplift at the surface is purely related to poroelasticity (Figure 2d) as only a small area above the reservoir is heated up and the impact of the caused themoelastic uplift dissipates within the first few hundred meters above the reservoir. From these findings, it can be concluded that injection pressure related poroelasticity is the main cause of surface uplifts, whereas the thermoelasticity and the related injection temperature are rather negligible.

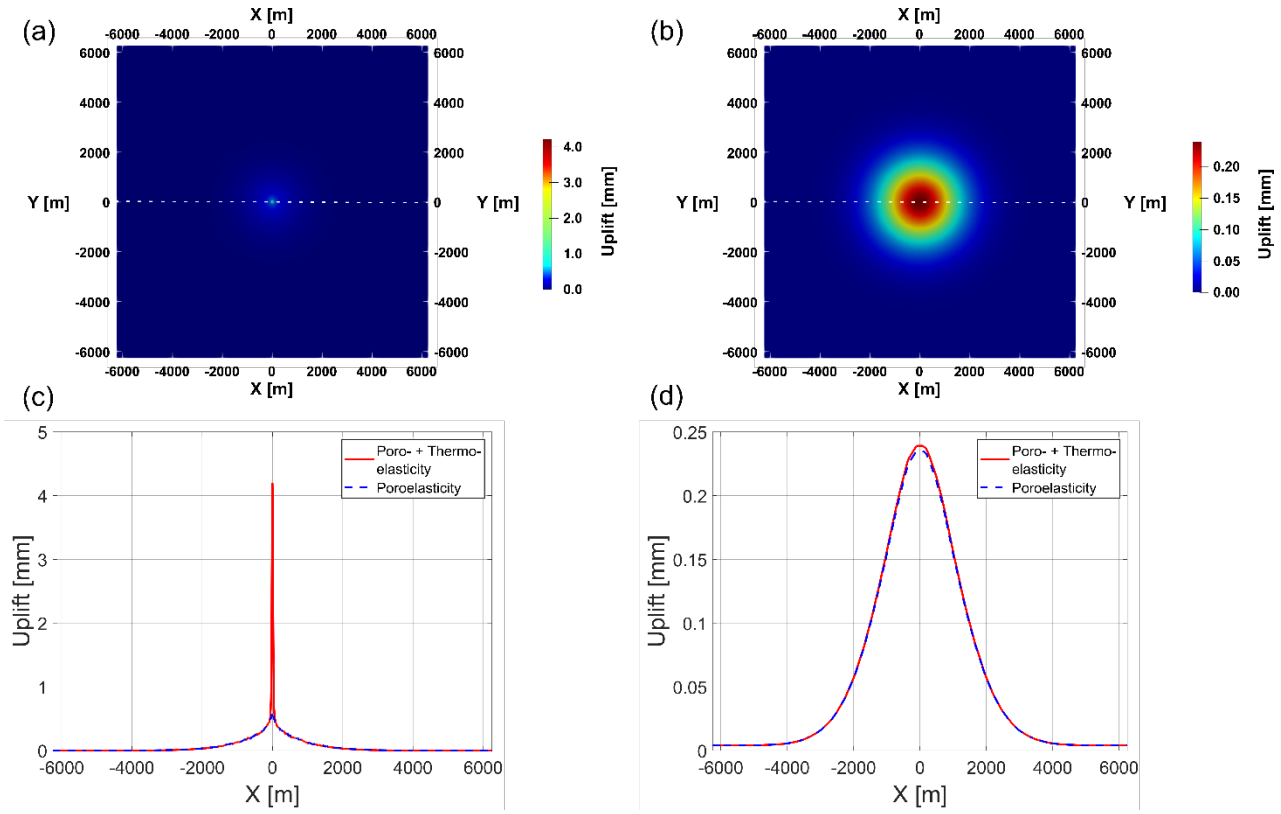

Figure 2: Distribution of the uplift after six months of injection in (a) a depth of 1195 m (top of the reservoir) and (b) at the top of the model (surface). Comparison of the uplift along the x-axis (at y = 0 m; dashed white lines in (a) and (b)) considering only poroelasticity (blue) and combining poro- and thermoelasticity (red) in (c) a depth of 1195 m (top of the reservoir) and (d) at the top of the model (surface).

The different impact of poro- and thermoelasticity is also visible in the distribution of the displacement at reservoir depth after the first production period of six months (after a total simulation time of one year; Figure 3).

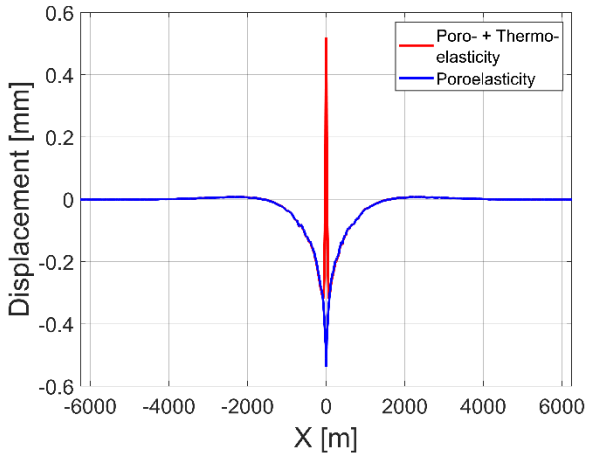

Figure 3: Distribution of the displacements after the first production period of six months (after a total simulation time of one year) at a depth of 1195 m (top of the reservoir).

For the case that only poroelasticity is considered, negative displacements of up to ca. 0.5 mm occur due to the pressure reduction caused by the production. This effect is strongly superimposed by the stress changes caused by the thermal disturbance around the well, which slowly decreases during the production period but does not reach the ambient reservoir conditions. Thus, a residual uplift of ca. 0.5 mm can be observed in the proximity of the well even after the production period.

At the surface, similar to the observations after six months of injection, there are no differences between pure poroelasticity and the fully-coupled THM simulation. After the production period, a maximum subsidence of ca. 0.1 mm occurs close to the well.

Thermohydraulic modelling of cyclic heat storage has proven that the reservoir heats up over time with each injection/production cycle. This is caused by diffusive, radial heat transfer around the well as the temperature of the injected water exceeds the ambient reservoir temperature (e.g. Kim et al. 2010, Stricker et al. 2020). This continuous heating of the reservoir also impacts the stress distribution in the reservoir. Figure 4 shows that if only poroelasticity is considered (blue circles), the negative displacements at the top of the reservoir show a quasi-steady behaviour and decrease only slightly over time.

However, when thermoelasticity is additionally taken into account, a strongly increasing thermoelastic effect (red circles) can be observed over time, resembling the continuous heating of the reservoir. The magnitude of the thermoelastic effect increases from ca. 1.1 mm after the first injection/production cycle to ca. 2.0 mm after ten cycles.

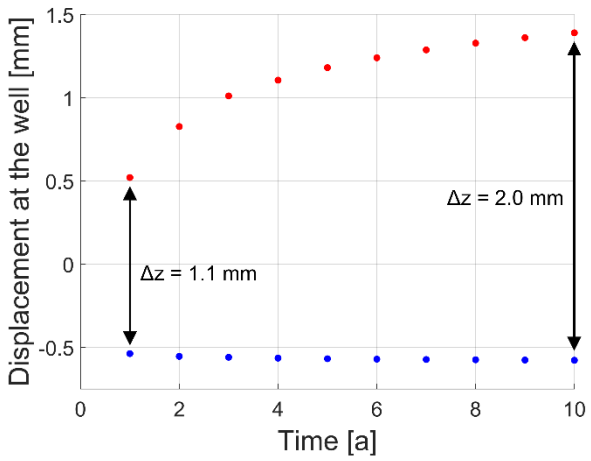

Figure 4: Temporal development of the displacement at the well in a depth of 1195 m (top of the reservoir). The blue dots represent a simulation with pure poroelasticity, whereas the red dots represent a simulation that additionally takes thermoelasticity into account.

At the surface where the influence of thermoelasticity is negligible, the magnitude of the subsidence does not change significantly over time. The subsidence appears to be only influenced by poroelasticity and increases slightly from 0.08 mm (after one year) to 0.10 mm, similar to the small increase of the subsidence at reservoir level for the case considering pure poroelasticity.

3. CONCLUSIONS AND OUTLOOK

Our simulations show that cyclic heat storage in deep reservoirs with moderate flow rates only leads to minor surface movements below one mm. These surface movements (especially the uplift during injection) are rather uniform, thus not leading to differential displacements over short distances that may cause damage to infrastructure elements above the storage site.

Our results further demonstrate the different impact of poroelasticity and thermoelasticity during cyclic injection and production. It becomes clear that displacements at reservoir depth are mainly caused by thermoelastic deformation due to hot water injection. The impact of thermoelasticity, however, is limited to a confined area around the well where the heating of the reservoir takes place. For this reason, injection-related uplifts at the surface are primarily driven by poroelasticity.

In future work, we want to build on these preliminary results by addressing more advanced research questions related to deep heat storage. As most HT-ATES systems are implemented using a well doublet, future modelling will be based on such a well setup, which can be expected to have even less impact on surface displacements (Birdsell and Saar 2020). Additionally, the model geometry should be adapted to resemble the geological conditions in the subsurface for the planned DeepStor research project in detail.

REFERENCES

Ausfelder et al.: “Sektorkopplung” – Untersuchungen und Überlegungen zur Entwicklung eines integrierten Energiesystems (Schriftenreihe Energiesysteme der Zukunft), München, 2017.

Baillieux, P.; Schill, E.; Edel, J.-B.; Mauri, G.: Localization of temperature anomalies in the Upper Rhine Graben: Insights from geophysics and neotectonic activity, Int. Geol. Rev., 2013, 55, 1744-1762.

Bear J.: Dynamics of Fluids in Porous Media, American Elsevier, New York, NY, USA, 1972. ISBN 978044401146.

Birdsell, D.T. and Saar, M.O.: Modeling Ground Surface Deformation at the Swiss HEATSTORE Underground Thermal Energy Storage Sites, Proceedings World Geothermal Congress, Reykjavik, Iceland, 2020.

Böcker, J: Petroleum System and Thermal History of the Upper Rhine Graben: Implications from Organic Geochemical Analyses, Oil-Source Rock Correlations and Numerical Modelling, Ph.D. Thesis, RWTH Aachen, Aachen, Germany, 2015.

Bruss, D.: Zur Herkunft der Erdöle im Mittleren Oberrheingraben und ihre Bedeutung für die Rekonstruktion der Migrationsgeschichte und der Speichergesteinsdiagenese, Ph.D. Thesis, Forschungszentrum Jülich/Universität Erlangen-Nürnberg, Jülich, Germany, 2000.

Dickinson, J.S.; Buik, N.; Matthews, M.C.; Snijders, A.: Aquifer thermal energy storage: Theoretical and operational analysis, Géotechnique, 2009, 59, 249-260.

Gao, L.; Zhao, J.; An, Q.; Wang, J.; Liu, X.: A review of system performance studies of aquifer thermal energy storage, Energy Procedia, 2017, 142, 3537-3543.

Geuzaine, C.; Remacle, J.-F.: Gmsh: A 3-D finite element mesh generator with built-in pre- and post-processing facilities, Int. J. Numer. Meth. Engng, 2009, 79, 1309-1331.

Gholami Korzani, M.; Held, S.; Kohl, T.: Numerical based filtering concept for feasibility evaluation and reservoir performance enhancement of hydrothermal doublet systems, J. Pet. Sci. Eng., 2020, 106803.

IEA: Energy Technology Perspectives 2017. Catalyzing Energy Technology Transformations; IEA Publications, International Energy Agency, Paris, 2017.

Jaeger, J.C., Cook, N.G., Zimmerman, R.: Fundamentals of rock mechanics, Blackwell Publishing, Malden, MA, USA, 2007. ISBN: 9780632057597

Jahn, S.; Mrugalla, S; Stark, L.: F+E Endlagerung, Methodik und Anwendungsbezug eines

Sicherheits- und Nachweiskonzeptes für ein HAW-Enlager im Tonstein, Endlagerstandortmodell Süd (AnSichT), Teil II: Zusammenstellung von Gesteinseigenschaften für den Langzeitsicherheitsnachweis, Bundesanstalt für Geowissenschaften und Rohstoffe, Hannover, Germany, 2016.

Jin, W.; Podgorney, R.; McLing, T.: THM coupled numerical analysis of the geothermal energy storage & extraction in porous fractured reservoir, 54th US Rock Mechanics/Geomechanics Symposium, Golden, Colorado, USA, 2020.

Kim, J.; Lee, Y.; Yoon, W.S.; Jeon, J.S.; Koo, M.-H.; Keehm, Y.: Numerical modelling of aquifer thermal energy storage system, Energy, 2010, 35, 4955-4965.

Lee, K.S.: Underground Thermal Energy Storage, Springer, London, UK, 2013. ISBN 978-1-4471-4273-7.

Marschall, P. and Giger, S.: Technischer Bericht 14-02, Geologische Grundlagen, Dossier IV Geomechanische Grundlagen, Nationale Gesellschaft für die Lagerung radioaktiver Abfälle (Nagra), Wettingen, Schweiz, 2014.

Permann, C.J.; Gaston, D.R.; Andrs, D.; Carlsen, R.W.; Kong, F.; Lindsay, A.D.; Miller, J.M.; Peterson, J.W.; Slaughter, A.E.; Stogner, R.H.; Martineau, R.C.: MOOSE: Enabling massively parallel multiphysics simulation, SoftwareX, 2020, 11, 100430.

REN21: Renewables 2019 Global Status Report, 2019. Available online: https://www.ren21.net/wp-content/uploads/2019/05/gsr_2019_full_report_en.pdf

Stricker, K.; Grimmer, J.C.; Egert, R.; Bremer, J.; Gholami Korzani, M.; Schill, E.; Kohl, T.: The Potential of Depleted Oil Reservoirs for High-Temperature Storage Systems, Energies, 2020, 13, 6510.

Wesselink, M.; Liu, W.; Koornneef, J.; van den Broek, M.: Conceptual market potential framework of high temperature aquifer thermal energy storage – A case study in the Netherlands, Energy, 2018, 147, 477-489.

Wirth, E.: Die Erdöllagerstätten Badens, Abh. Geol., 1962, 4, 81-101.

Acknowledgements

This study is part of the subtopic “Geoenergy” in the program “MTET – Materials and Technologies for the Energy Transition” of the Helmholtz Association. The authors are responsible for the content of this publication.